Available online http://amq.aiqua.it
ISSN (print): 2279-7327, ISSN (online): 2279-7335

Alpine and Mediterranean Quaternary, 35 (2), 2022, 1-16 https://doi.org/10.26382/AMQ.2022.07

THE TICINO-TOCE ICE CONVEYOR BELTS DURING THE LAST GLACIAL MAXIMUM.

Giovanni Monegato [1], Sarah Kamleitner [2], Franco Gianotti [3], Silvana Martin [4], Cristian Scapozza [5], Susan Ivy-Ochs [2]

[1] Institute of Geosciences and Earth Resources, National Research Council, Padova, Italy.
[2] Laboratory of Ion Beam Physics, ETH Zurich, Zurich, Switzerland.
[3] Dipartimento di Scienze della Terra, Università di Torino, Torino, Italy.
[4] Dipartimento di Geoscienze, Università di Padova, Padova, Italy.
[5] Istituto scienze della Terra, Scuola Universitaria Professionale della Svizzera Italiana SUPSI, Mendrisio, Switzerland.

Corresponding author: G. Monegato <giovanni.monegato@igg.cnr.it>

ABSTRACT: The provenance and distribution of erratic boulders of the Ticino-Toce glacier network yields key information for determining glaciers' paleoflow and highlights the interaction between two major Alpine glacier systems during the Last Glacial Maximum (LGM). Boulders in the central and western parts of the Verbano, as well as in the smaller Orta end moraine systems, originate from the Toce catchment. Erratics pertaining to the Ticino mountain basin characterize the eastern flank of the Verbano amphitheatre and the glacial deposits in the Ceresio system. The wide distribution of Toce lithologies in the Verbano end moraine system can, despite its smaller overall size, be ascribed to the hypsometry and valley course of the Toce catchment. Areas with highest-elevation (>4000 m a.s.l.) and a short flow path (<100 km), favored the early spread of the Toce glacier. In the first phase of the LGM, the preceding advance of the Toce glacier may have suppressed the larger, possibly inert, Ticino glacier towards the east forcing its diffluence into the prealpine area of Ceresio, which had no local glaciers and was likely impacted by a western branch of the Adda glacier. The dynamics of the Ticino-Toce glacier network during the LGM highlight the role of the topography and location of the accumulation areas in driving differential development of glaciers originating from high catchments that can force nearby glaciers with greater inertia towards a different path.

Keywords: European Alps, Last Glacial Maximum, palaeoglacier, erratic boulder, provenance.

1. INTRODUCTION

Glacial dispersal trains (Shilts, 1982) - i.e. trails of deposits and clasts eroded from a bedrock source, transported downglacier and deposited in the stratigraphic record (Cummings & Russell, 2018) - represent an important tool for understanding the flow of glaciers and the delivery of glacigenic sediments, including the distribution of particular types of rocks or minerals in the glacial till (e.g., Shilts, 1993; McClenaghan et al., 2001). Empirical tests in tills of boreal ice sheets (e.g., Larson & Mooers, 2004) highlight the key role that distance from the source areas plays in the downflow distribution of the indicator lithotypes in glacigenic deposits. In glaciated mountains the dispersal train largely follows the major valleys towards the piedmont plains. Gravitational processes (e.g., rock fall, slope failures) occurring at the interface of the glacier and the ice-free valley slopes promote debris accumulation and its consequent embedding into the ice (e.g., Evans, 2003; Goodsells et al., 2005). Supraglacial delivery - including large (erratic) boulders - represents a peculiar characteristic of mountain glaciers. Erratic boulders evidence past glacier extents, even where no till can be found. They are key to inferring the pathways and transfluences within the network of valley glaciers that developed in the Alps during Pleistocene glaciations (e.g. van Husen, 2004; Kelly et al., 2004; Bini et al., 2009).

Understanding the dynamics of large mountain glaciers during Pleistocene glaciations is intriguing because present-day analogs are scarce and located at different latitudes (i.e. Alaskan Range or Patagonian Andes) or at different elevations (Himalaya). Modern glaciers with piedmont lobes are very rare and limited to the Alaskan Range, Kunlun Mountains and Iceland. Consequently, a multidisciplinary approach is needed to reconstruct the functioning of past Alpine ice-stream networks. For the European Alps, the excellent knowledge on Last Glacial Maximum (LGM) glacier extent has fostered numerous glacier modelling studies and related ELA interpretations (Becker et al., 2016; Jouvet et al., 2017; Cohen et al., 2018; Seguinot et al., 2018; Imhof et al., 2019; Višnjević et al., 2020; Seguinot & Delaney, 2021; Del Gobbo et al., 2022). Modelling results additionally provide information on paleoglacier velocity, sliding, thickness and flow path. Even if the simulations show certain discrepancies with the sedimentological and geomorphological data with regard to glacier extent and ice thickness, they raise important questions about ice development during major glaciations and the building of interconnections among the valley glaciers (Bini et al., 2009; Seguinot et al., 2018).

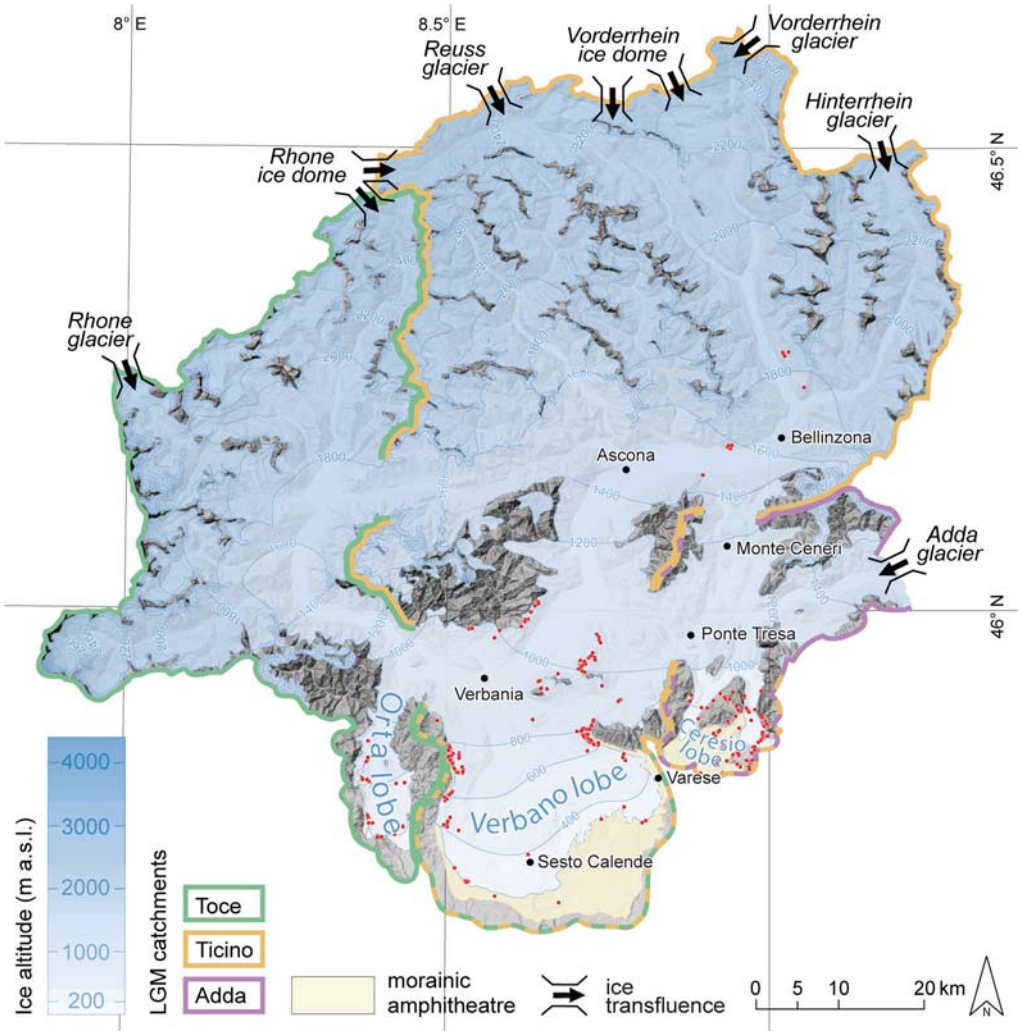

Fig. 1 - Extent of the LGM Ticino-Toce glacier system (modified after Bini et al. 2009, Braakhekke et al., 2020 (Orta lobe), Kamleitner et al., 2022a (Verbano lobe)). Red dots represent erratic boulders included in different studies (Bernoulli et al., 2018; Braakhekke et al., 2020; Kamleitner et al., 2022a).

Reconstructions based on geomorphological/geological data become more difficult moving from the outer sectors of the chain, where piedmont lobes spread onto the plain, to the axial sector, where the accumulation areas were located. In this inner portion of the cathement the landforms related to the glacial maxima are scarce, while glacigenic sediments are present but hardly useful for paleoglacier reconstruction. A key tool for understanding the flow of paleoglaciers and their possible interconnections through transfluences is the provenance of glacial debris and particularly that of erratic boulders carrying the lithological signature of the source catchment (e.g., Coutterand et al., 2009; Coutterand, 2010; Jouvet et al., 2017; Braakhekke et al., 2020). Large erratic boulders are more suited than smaller clasts for such a task as they are large enough to barely suffer from the possible bias of reworking, as their datings to the LGM have shown (see section Materials and Methods). While not every type of rock can produce big boulders, those boulders transported on the ice surface would not suffer from mixing and would generally remain on the side of the glacier that they fell onto. An exception in this assumption is related to large landslides, which may scatter the debris across the whole width of the flowing glacier (e.g., Menzies et al., 2017; Frasca et al., 2020). Boulder roundness can additionally inform about the transport position (supraglacial or subglacial). The potential of using erratic boulders to model glacier flow was shown by several studies (Florineth & Schlüchter, 1998; Jouvet et al., 2017; Cohen et al., 2018), yet the coupling with chronology is critical. Through field studies and different absolute dating techniques, the chronology of the Alpine LGM has been refined over the last decades, allowing to depict the LGM ice margin in several sectors of the mountain range (Monegato et al., 2007, 2017; Reber et al., 2014; Scapozza et al., 2014; Gianotti et al., 2015; Bernoulli et al., 2018; Ivy-Ochs et al., 2018; Braakhekke et al., 2020; Kamleitner et al., 2022a; Kamleitner et al., 2022b).

The present study shows the reconstruction of the paleo-ice streams of the Ticino-Toce glacier system (Fig. 1), one of the largest paleoglaciers in the central southern

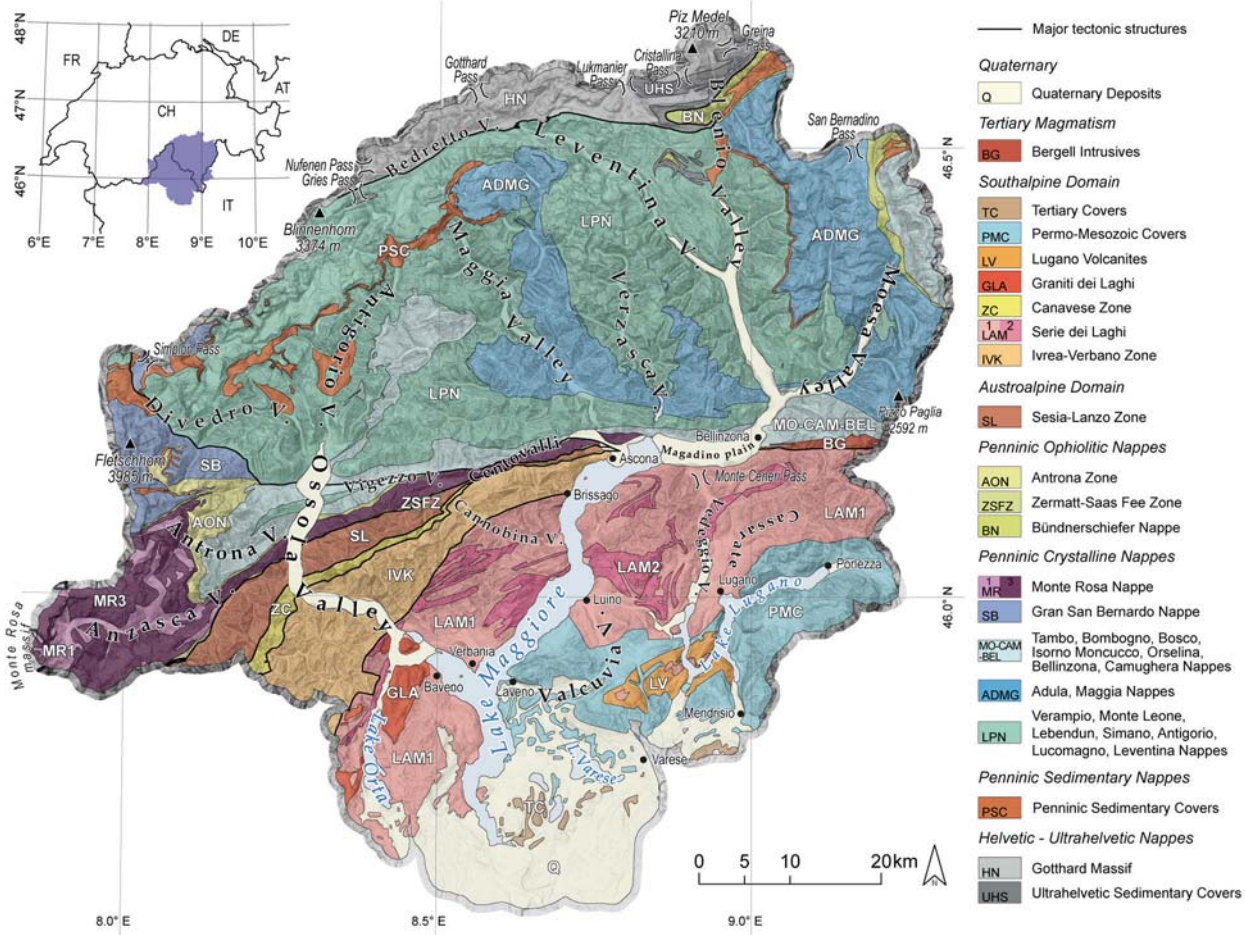

Fig. 2 - Geological Map of the Ticino-Toce catchment. Data synthesized from swisstopo (2005).

Alps, and possibly interconnections with neighboring catchments of Rhone, Reuss, Rhine and Adda. The LGM chronology of the Ticino-Toce glacier system was recently assessed by the means of exposure dating of erratic boulders and geomorphological considerations (Braakhekke et al., 2020; Kamleitner et al., 2022a). This allowed to reconstruct the shape of the Orta and Verbano piedmont lobes in detail (Fig. 1). Evaluating the boulders' source areas may allow to infer the flow lines of the Ticino-Toce ice streams and test existing glacier models (Seguinot et al., 2018), which suggest asynchrony in the development between the Ticino and the Toce valley glaciers.

2. STUDY AREA

The Ticino-Toce catchment is about 6700 km^2 in size and located in the Western Alps, south of the main Alpine divide. The drainage basin is characterized by an unequal distribution of elevation (Fig. 1, Fig. 2). The highest peaks are located at the western boundary along Monte Rosa-Fletschhorn line with elevations up to above 4600 m a.s.l. Whereas, the northern and especially the eastern sectors have accumulation areas below 3500 m a.s.l. The southern parts of the catchment are characterized by several valley reaches, some filled by lakes. The longitudinal profiles of the valleys illustrate the asymmetry between the Toce and Ticino catchments, with the former being characterized by high gradients and the latter by longer reaches (Fig. 3). The Ticino and Toce valleys are overdeepened (Preusser et al., 2010), with the base of bedrock reported at 600 m b.s.l. at the Magadino plain, progressively decreasing to maximum basin depth of 800 m b.s.l. halfway between Luino and Laveno (Cazzini et al., 2020). The overdeepening of these valleys, similarly to other valleys on the southern flanks of the Alps, is assumed to have formed during the Messinian Salinity Crisis (Bini et al., 1978, Finckh, 1978, Hantke, 1983). Debris flow, fluvial and fluvio-deltaic sediments of Messinian age (Miocene), as well as marine sediments of Zanclean age (Pliocene), were indeed observed in the valleys between Mendrisio (southern Switzerland) and Varese (northern Italy) (Bernoulli et al., 2018). Nevertheless, this interpretation is debated and a glacial origin of the upstream sections of southern Alpine valleys is currently proposed (Winterberg et al., 2020). The lake bottom at the outlet of the Ossola Valley does not show a fluvial incision and, during the Messinian, the Toce River was inferred to have flowed into the Orta Valley (Cazzini et al., 2020),

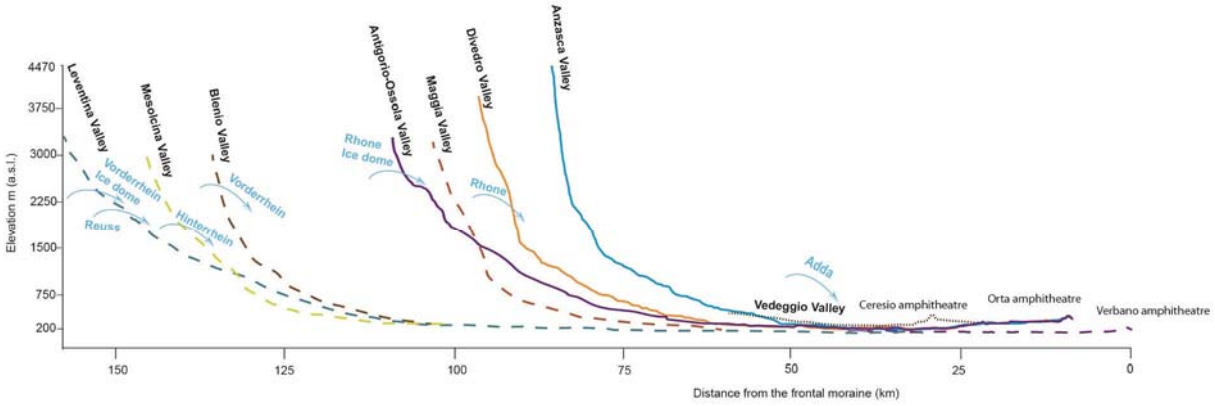

Fig. 3 - Longitudinal profiles of the major valleys; those related to the Toce catchment are in solid lines, those of the Ticino catchment in dashed lines; in dotted line the Vedeggio Valley related to the transfluence towards the Ceresio morainic amphitheatre. Blue arrows show the elevation of the major transfluences from the respective glaciers. Longitudinal distance from the outern LGM moraines of the Verbano according to Kamleitner et al. (2022a).

where the bedrock crops out underneath the frontal moraines of the Orta end moraine system (Braakhekke et al., 2020).

2.1. Geological setting

The bedrock of the Ticino-Toce mountain basin (Fig. 2) can be split into two major domains (Dal Piaz, 2010): (a) the Southalpine domain with a Paleozoic basement and the Permo-Mesozoic sedimentary covers, both lacking Alpine metamorphism; (b) the second domain was affected by Alpine metamorphic phases that include: the Sesia-Lanzo Zone (SL), the Penninic and the Helvetic nappes. The second domain is characterized by a stack of basement and cover nappes with high -pressure Alpine metamorphism of Late Cretaceous - Eocene age and a Late Eocene-Early Oligocene greenschist to amphibolite facies overprinting (Lepontine Dome: Frey et al., 1999). The two domains are separated by the Periadriatic/Insubric lineament, a 1000 km long post-collisional transpressive fault with post-Late Oligocene to Miocene activity.

The valleys of Lake Orta and Lake Maggiore are situated in the Southalpine domain (Fig. 2) dominated by Palaeozoic metamorphic rocks called Massicio dei Laghi (MdL), by late Variscan volcanic suites and Permo-Mesozoic sedimentary covers at the outlets and east of Lake Maggiore (see Geological Map of Switzerland, 1:500,000; Federal Office of Topography swisstopo 2005; Piana et al., 2017). The Alpine metamorphism is interpreted to have had only minimal effects on the MdL (Rutter et al., 2007), whose main metamorphism is of Caledonian (Late Cambrian-Early Devonian) to Variscan (Late Devonian-Early Permian) age (Boriani et al., 1990a; Pinarelli et al., 1993). The MdL is divided into the Ivrea-Verbano Zone (IVK) and the Serie dei Laghi (LAM) separated by the Cossato-Mergozzo-Brissago (CMB) tectonic line (Fig. 2). The Ivrea-Verbano Zone (IVK) is one of the most spectacular sections through lower continental crust, including the mantle peridotite series, which was tilted vertically and brought to the surface during Alpine orogenesis (Rutter et al., 2007). A thick sequence of high-grade metapelitic schists referred to as the “Kinzigite” formation, intruded by gabbro and diorite plutons at the mantle-crust boundary. These "Kinzigite" schists contain mainly garnet, biotite, plagioclase, quartz, sillimanite and possible muscovite (Rutter et al., 2007). Early Permian granites (named Graniti dei Laghi, GLA) intruded the LAM (i.e. plutons of Mottarone and Montorfano). These plutons are unaffected by Alpine metamorphism (Boriani et al., 1990b). The Prealps east of Lake Maggiore are largely characterized by sedimentary covers of the southalpine domain (Bertotti et al., 1993). These are Permo-Mesozoic (PMC) to Tertiary (TC) shelf to basin marine formations. Lugano Volcanites (LV) outcropping on the left side of the Valcuvia Valley are of Permian age (Hunziker & Zingg, 1980).

The Insubric Line is crosscut by the Toce Valley and the Ticino Valley in the W-E reach of Lake Maggiore (Fig. 2). Here the narrow (about 2 km wide) Canavese Zone (ZC; Southalpine domain) is in tectonic contact with the Ivrea-Verbano and Sesia-Lanzo zones to the south and north, respectively. The Canavese Zone includes many types of rocks, such as gneisses, schists, Permian diorite, serpentinites and sedimentary carbonate and siliceous rocks, that are locally strongly deformed, with a low-grade Alpine metamorphism (Ferrando et al., 2004). West of Bellinzona the tail of the Bergell pluton (BG) is characterized by tonalite (Schmid et al., 1996).

The Sesia-Lanzo Zone (SL) is the first unit showing Alpine metamorphism (Compagnoni et al., 1977). It is composed of rocks derived from the Southalpine domain and forming the distal edge of the Adria microplate before the Alpine collision (Austroalpine domain). SL was subdivided by previous authors into: “Gneiss Minuti”, “Micascisti eclogitici” and “II Zona Diorito-kinzigitica”

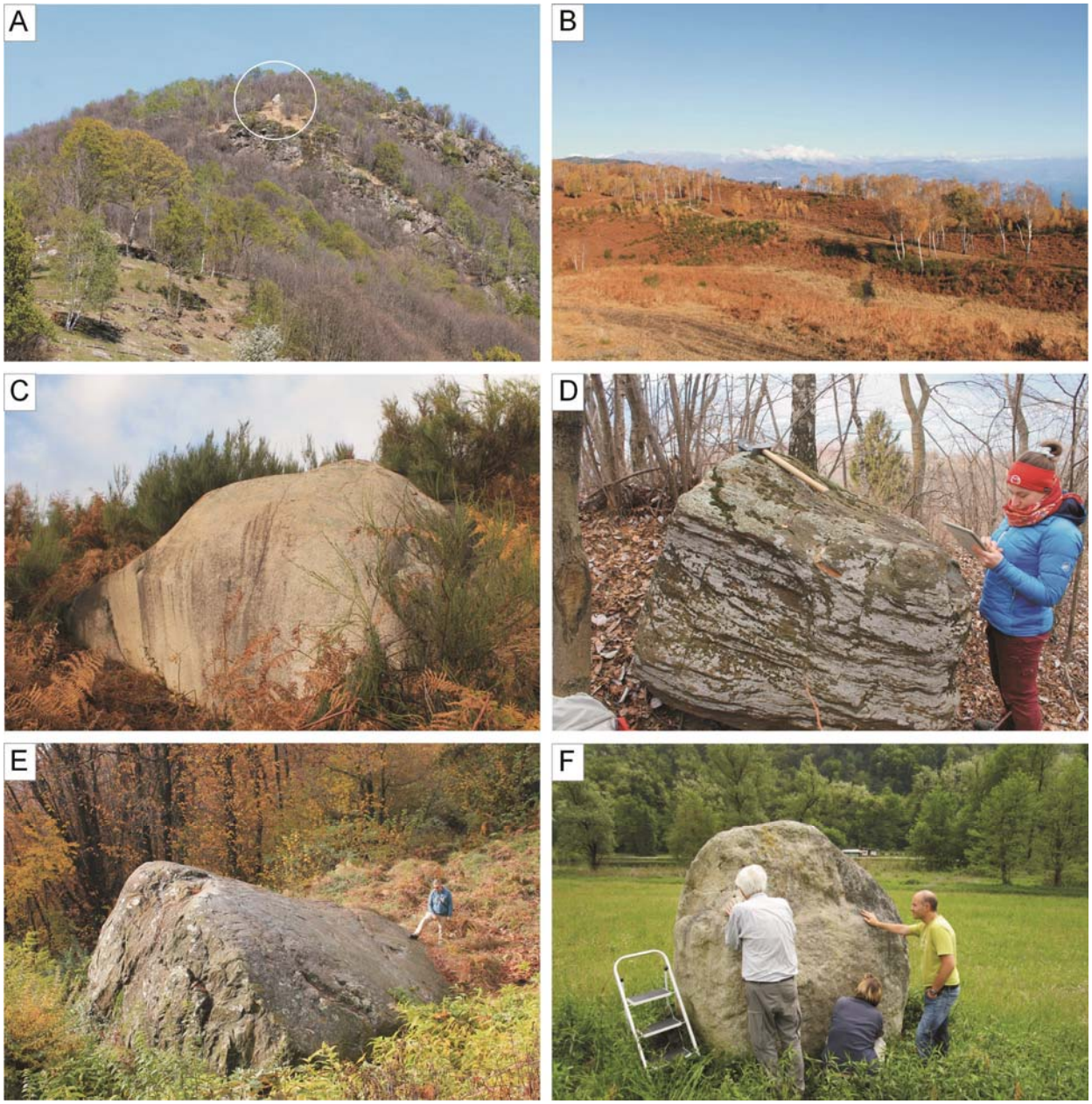

Fig. 4 - Photos of glacial landforms and erratic boulders (see Table 2) from the Ticino-Toce systems: A) boulder Puffer 11 made of IVK gneiss resting on a rocky relief (right slope of Lake Orta); B) impressive group of seven right lateral moraines of the Verbano glacier lobe on the watershed between the Lake Maggiore and Lake Orta basins, supporting many granite boulders (Alpe Canà); C) sub-rounded boulder VR30 made of GLA white granite, which provided a pre-LGM ^{10}Be age (Alpe Canà moraines; Kamleitner et al., 2022a); D) small angular boulder VR37 made of LAM1 garnet paragneiss (S. Michele, eastern slope of Lake Maggiore, NW of Laveno); E) big polished sub-angular boulder VR22 made of AON serpentinite (Alpe Pala at Miazzina on the western slope of Lake Maggiore); F) Velmaio Megalith Invorio Breccia (PMC Breccia). Other photos of erratic boulders from the Orta basin (Bugnate 17-18, Grassona 25, Briallo 33, Carcegna 50, Colma 20 and Armeno 39) are found in Braakhekke et al. (2020). Photos of boulders VR16, VR31, VR45-46 and VR51-52 from the Verbano system are found in Kamleitner et al. (2022a).

bordered by a southern marginal shear belt. “Gneiss Minuti” are albite-white mica gneisses and schists, with a local porphyroclastic texture. Locally, "Gneiss Minuti" complex contains coarse-grained metagranitoids. “Micascisti eclogitici” are made of high-pressure (eclogite to blueschist facies) micaschists with jadeitic pyroxene-garnet + glaucophane + chloritoid with intercalated eclogites, glaucophane metabasites and marbles. The term "kinzigite" is used in the Alpine literature for indicating high-grade (amphibolite facies) sillimanite-

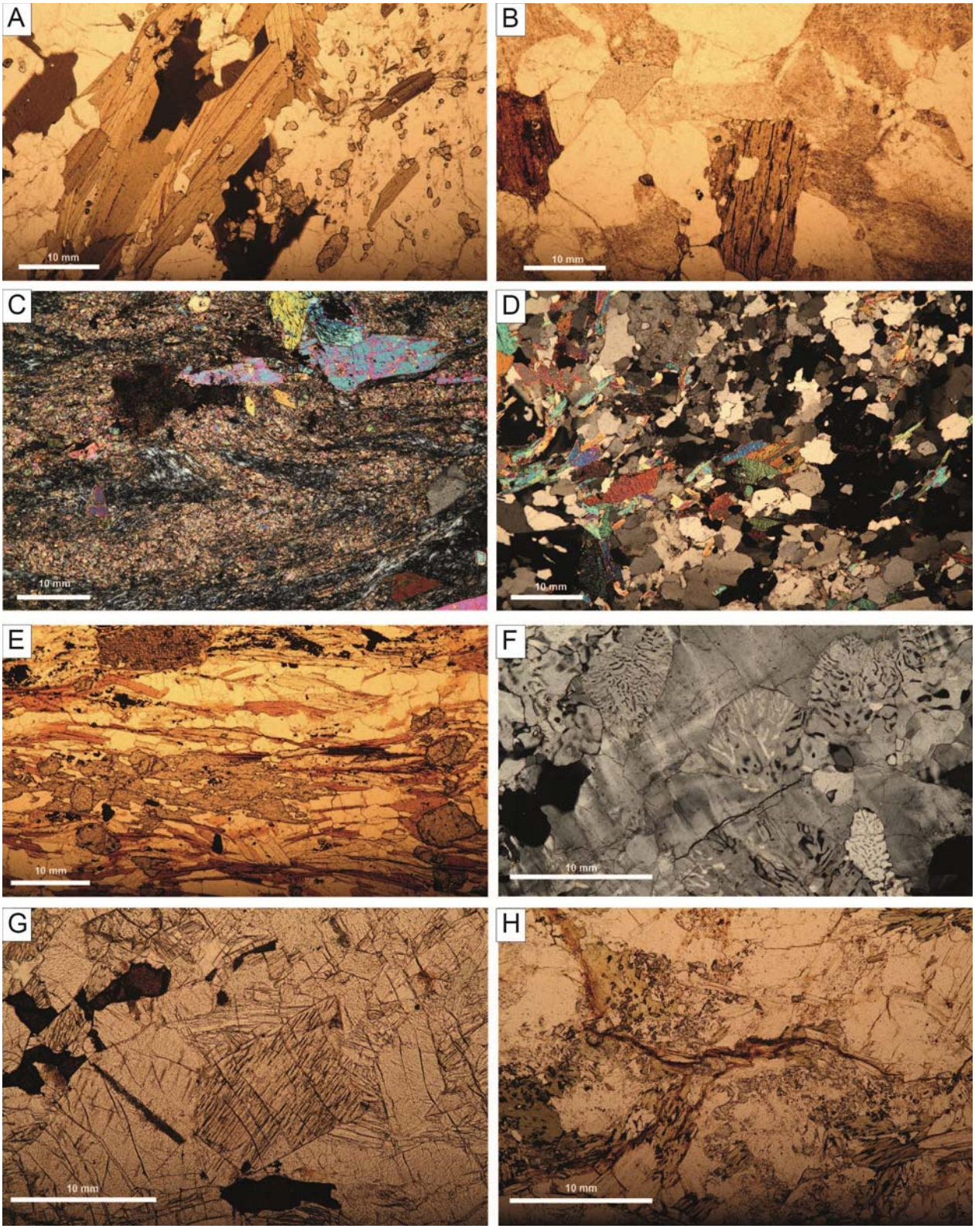

Fig. 5 - Plate of thin section samples (see also Table 2): A) VR23, green biotite orthogneiss (LAM2); B) VR14, granite (GLA); C) VR02, serpentinite (AON); D) VR39, paragneiss (LAM1); E) VR37, garnet paragneiss (LAM1, Fig. 4D), F) VR24, green biotite orthogneiss with myrmekite (LAM2); G) VR20, granulite (IVK); H) VR27, garnet orthogneiss (MR1).

garnet-biotite gneisses of the IVK and of the "II Zona Diorito-kinzigitica". The SL crops out in the lower Ossola Valley for about 4 km at the Anzasca-Toce confluence, while it pinches out in the Ticino Valley near Ascona (Fig. 2).

In the north-western sector, the topmost Penninic nappe is the Zermatt-Saas Fee Zone (ZSFZ), which forms a very thin and discontinuous oceanic crust slice in the Toce basin (Fig. 2). It is predominantly composed of serpentinized ultramafites, associated to mafic rocks (metagabbros, metavolcanites and metasediments) crystallized under high-pressure conditions. Towards the east, the ZSFZ pinches out at the northern tip of Lake Maggiore.

The Monte Rosa (MR) is an Upper Penninic continental unit characterized by a large SW-vergent recumbent antiform (Berger et al., 2011) with a core composed of high-pressure micaschists and "gneiss minuti" derived from high-grade Paleozoic paragneiss (MR1, Piana et al., 2017) cropping out along the Anzasca Valley bottom (Fig. 2) and a shell composed of dominant metagranitoid (MR3, Frey et al., 1976; Piana et al., 2017). These are characterized by K-feldspar megacrystals up to ten centimeters in size, preserved within the Alpine schistosity. Monte Rosa "gneiss minuti" are characterized by albite, fine-grained quartz, white mica, chlorite and garnet. In the micaschists, high-pressure assemblages include chloritoid, phengite, garnet with kyanite, talc, Mg-chlorite and glaucophane. The Alpine high-pressure assemblages are overprinted by a greenschist Tertiary metamorphism (Keller et al., 2005) as shown by crystallization of biotite from white mica, albite blastesis (poikiloblasts) and quartz recrystallization to form homogeneous coarse-grained aggregates.

The Antrona metaophiolite (AON) is a nappe of oceanic crust interposed between the overlying Monte Rosa and the underlying Camughera and Moncucco nappes (Bigioggero et al., 1981). It crops out on the left side of Anzasca Valley and more extensively in the upper Antrona Valley (Fig. 2). The AON suite includes serpentinized ultramafites, metagabbros and metabasites (Turco & Tartarotti, 2006). Eclogite metabasite with garnet, amphibole and relict omphacitic clinopyroxene are described by Colombi & Pfeifer (1986) in the Antrona and Anzasca valleys.

Middle Penninic unit to the west (Toce catchment) is the Gran San Bernardo (SB). In the central eastern to the eastern sectors of the Ticino-Toce mountain basin the Middle Penninic units are characterized by greenschist facies paragneiss and orthogneiss with blueschist relics (Bigi et al., 1983). They were grouped (MO-CAM-BEL) in the geological map of Figure 2. The Moncucco-Orselina (MO) and Camughera (CAM) are folded together with AON, MR and ZS units. They show a medium-grade metamorphic overprinting by the Lepontine metamorphism (Keller et al., 2005). CAM is made of micaschists derived from mid- to high-grade Paleozoic gneisses (paragneiss, orthogneiss, amphibolites) and dominant metagranitoids similar to those of MR3, with Alpine high-pressure overprint. MO is composed of a Paleozoic basement covered by Permo-Carboniferous sequences including graphitic schists, basic metavolcanites and Permian sub-volcanic bodies, suggesting affinity with the Gran San Bernardo nappe (Bigioggero et al., 1981). Tambo, Bosco and Bellinzona nappes are made of Paleozoic basement and slices of Mesozoic covers and Bundner schist (Baudin et al., 1993). Their lithological setting is similar to that of the Monte Leone nappe (Maxelon & Mancktelow, 2005). Tambo, Bosco, Bellinzzona and Monte Leone nappes are recrystallized under amphibolite facies (biotite, staurolite, garnet).

The deep Penninic nappes (Monte Leone, Lebendun, Simano, Lucomagno, Leventina, Antigorio and Verampio, LPN) show a strong Lepontine amphibolite facies metamorphic overprint. It is characterized by crystallization of new minerals over the early Alpine metamorphism (Bigioggero et al., 1981; Berger et al., 2011). The LPN are composed of a typical Paleozoic basement (paragneisses, orthogneisses, amphibolites), with late Paleozoic intrusions and Permo-Carboniferous to Mesozoic sequences similar to the other Penninic nappes. These units characterize the innermost sectors of Ticino and Toce catchments (Fig. 2).

The Ultra-Helvetic Mesozoic cover sequences and the Helvetic Gotthard basement (HN), including the Permian granitoids (Sergeev & Steiger, 1995), make up the far northern part of the Ticino mountain basin (Fig. 2).

2.2. The LGM Ticino-Toce glacier system

The Ticino-Toce accumulation area is located south of the major Rhone and Rhine (or Vorderrhein) ice domes (Fig. 1; Kelly et al., 2004; Bini et al., 2009). In the inner Alpine accumulation areas, additional input of ice could have been added to the Ticino basin (4900 km^2) by overflowing of the Rhone ice dome to the East along Bedretto Valley via Nufenen Pass (Fig. 2). In Leventina Valley, the Ticino glacier received large ice masses built up in the high-mountain cirques of Gotthard Pass. Downstream of Leventina Valley, Ticino trunk glacier was joined by ice draining Blenio and Moesa valleys. Both tributaries were influenced by likely transfluences from the Vorderrhein ice dome via Lukmanier, Cristallina and Greina passes, as well as from the Hinterrhein accumulation areas via San Bernardino Pass (Fig. 2). Right tributary glaciers of Verzasca and Maggia valleys fed the Ticino glacier together with Toce ice overflowing through Centovalli Valley. On the left side of the Ticino Valley, another diffluence existed over Monte Ceneri Pass, draining ice directly to the south and towards Lugano. In parts, these ice masses united with ice outflowing the Adda glacier systems and terminated in the small Ceresio lobe south of Lake Lugano (Fig. 1; Bini et al., 2009). Through an overspill located near Ponte Tresa, some of the drained ice also re-entered the Ticino catchment at Valcuvia Valley (Bini et al., 2009) and merged with the united Ticino-Toce glacier at the western slope of the Campo dei Fiori (Fig. 1, see Fig. 6). Advancing southwards, the large Ticino valley glacier filled the overdeepened basin of Lake Maggiore (Preusser et al., 2010) and merged with Toce glacier coming in from the northwest.

In its upper parts, the smaller Toce catchment (~1800 km^2) was dominated by ice draining through Divedro- and Antigorio valleys, two tributary glaciers with additional linkage to the Rhone glacier system adjacent

in the north (Fig.1, Fig. 2). The Toce glacier system received overflowing ice from the Rhone valley glacier via Simplon Pass and through a direct link to the Rhone ice dome (Florineth & Schlüchter, 1998; Kelly et al., 2004). An ice diffluence existed in the middle of the Ossola Valley, where ice of the Toce catchment did overflow into the Ticino catchment along the western Vigezzo Valley (a tributary of Toce Valley) and the Centovalli Valley (a tributary of Ticino Valley). Right tributary glaciers of Antrona and Anzasca valleys joined the Toce trunk glacier downstream. Originating in the eastern slope of the Monte Rosa, ice outflowing Anzasca Valley represented the major tributary glacier. Downstream from the Anzasca confluence, one part of the Toce glacier branched off to the south into the Orta Valley, building up the correspondent Orta glacier lobe (~85 km^2 in area) and a small morainic amphitheater (Novarese, 1927; Braakhekke et al., 2020). The main branch of the Toce glacier, however, continued to the southeast to merge with the Ticino glacier.

Downstream of the confluence at the Gulf of Borromeo, between Stresa and Verbania, the merged Ticino-Toce glacier filled the basin of Lake Maggiore and advanced several kilometers (about 28 km) towards the SSE (Fig. 1, Fig. 2). The topographic control was reduced and the LGM Ticino-Toce piedmont lobe terminated on the plain. The bulbous terminus (known as Verbano lobe) spread to cover ~380 km^2 (Kamleitner et al., 2022a). Pre-LGM and LGM advances of the Ticino-Toce glacier built up a multi-ridged, closely stacked end moraine system, interlaced and succeeded by glaciofluvial plains (Bini et al., 2014; Piana et al., 2017; Bernoulli et al., 2017; Kamleitner et al., 2022a). The LGM maximum advances of both, Orta and Verbano lobes, were recently dated to ca. 25 ka and are interpreted to have been followed by a several thousand-year long period of glacier fluctuations near the maximum position (Braakhekke et al., 2020; Kamleitner et al., 2022a). Late LGM readvances (~20-19 ka) were likely followed by rapid ice decay and retreat from the foreland (Braakhekke et al., 2020; Kamleitner et al., 2022a).

The occurrence of large erratic boulders within the Orta and Verbano morainic amphitheatres was stated by several authors since the 19th century (Omboni, 1861; Gentilli, 1866; Salmojraghi, 1882; Sacco, 1892; CAI, 1914). The biggest erratics were quarried for building purposes already in prehistory (De Marinis,

>>>>>

Tab. 1 - Details of erratic boulders of the Orta-Verbano and Ceresio systems lithologically analysed in this study.

Name	roundness	Lithology	Geological unit	Size (m)		altitude		Coordinates	
				Length	Width	Height	m a.s.l.	°N	°E
VR53	SR	Paragneiss	ADMG	5,0	3,0	1,5	650	45,869	8,709
VR55	AN	Orthogneiss	ADMG	2,5	1,5	1,3	700	45,866	8,720
ER132	SR	Garnet micaschist	ADMG	2,0	2,5	3,0	698	45,919	8,741
VR02	SA	Talcschist	AON	5,0	4,0	2,0	488	45,769	8,502
VR04	AN	Prasinite	AON	3,0	2,0	1,0	642	45,797	8,502
VR22	SA	Serpentinite	AON	7,0	5,0	5,0	880	45,979	8,534
VR33	AN	Serpentinite	AON	1,9	1,6	1,5	613	45,796	8,502
VR51	AN	Serpentinite	AON	8,0	3,0	6,0	336	45,707	8,531
VR52	SA	Serpentinite	AON	13,0	10,0	4,0	343	45,691	8,576
ER192	AN	Tremolitite	AON	2,0	1,7	0,9	390	45,774	8,740
Briallo 32	AN	Amphibolite	AON	2,0	1,2	1,5	500	45,775	8,380
Bugnate 17	SA	Metabasite	AON	5,0	3,0	1,2	522	45,753	8,394
ER191	AN	Granodiorite	BG	4,0	2,8	1,9	306	45,788	8,776
GUDO01	SA	Granodiorite	BG	4,0	2,0	1,9	250	46,175	8,939
Armeno 39	AN	Garnet micaschist	CAM (MO-CAM-BEL)	5,0	4,0	5,0	504	45,813	8,436
Buccone 38	SR	Orthogneiss	CAM (MO-CAM-BEL)	1,3	1,0	0,7	416	45,765	8,434
VR14	SR	Granite	GLA	1,6	1,0	1,0	828	45,851	8,504
VR19	SR	Granite	GLA	3,0	1,0	0,8	868	45,880	8,486
VR28	SA	Granite	GLA	2,0	2,0	1,5	807	45,845	8,504
VR29	SR	Granite	GLA	3,5	2,5	1,9	806	45,844	8,504
VR30	SR	Granite	GLA	4,5	5,0	2,5	781	45,843	8,505
VR42	SR	Granite	GLA	1,6	1,4	1,4	802	45,845	8,504
VR43	SR	Granite	GLA	2,0	1,5	1,2	774	45,844	8,507
VR44	SR	Granite	GLA	3,0	1,0	1,3	803	45,845	8,506
VR45	SR	Granite	GLA	6,0	4,0	4,0	785	45,836	8,508
VR47	SR	Granite	GLA	1,8	1,2	1,1	736	45,841	8,504
Antenna 1	SR	Granite	GLA	2,5	2,0	2,0	596	45,814	8,381
Briallo 33	SA	Granite	GLA	4,0	2,2	1,5	517	45,778	8,379
Carcegna 50	SA	Granite	GLA	2,0	1,5	1,4	595	45,812	8,423
ME130	AN	Granite	GLA	0,7	0,5	0,9	408	45,823	8,890
VR36	SA	Metagranite	HN	2,5	2,5	1,2	1048	45,949	8,720
VR06	SA	Gabbro	IVK	6,0	3,0	3,0	648	45,802	8,508
VR20	SR	Granulite	IVK	1,5	2,0	2,5	888	45,980	8,539
ER01	SR	Granulite	IVK	5,0	4,0	5,0	344	45,762	8,523
ER186	SA	Paragneiss	IVK	-	-	-	355	45,706	8,535
Egro 28	SA	Orthogneiss	IVK	3,4	2,0	1,6	641	45,816	8,378
Grassona 24	AN	Kinzigite	IVK	8,4	1,5	1,8	539	45,816	8,371
Puffer 11	AN	Orthogneiss	IVK	4,0	3,0	2,5	657	45,858	8,379
VR15	AN	Paragneiss	LAM1	10,0	4,0	2,5	566	45,844	8,521
VR16	AN	Micaschist	LAM1	7,0	3,5	5,0	582	45,844	8,522
VR17	AN	Paragneiss	LAM1	2,5	1,7	1,2	575	45,845	8,522
VR18	AN	Garnet micaschist	LAM1	2,0	2,0	1,8	565	45,841	8,521
VR37	SA	Garnet gneiss	LAM1	2,0	1,5	1,5	839	45,943	8,711
VR39	AN	Paragneiss	LAM1	2,0	1,6	1,5	860	45,916	8,643
VR48	AN	Micaschist	LAM1	1,5	1,0	0,3	569	45,854	8,730
VR03	SR	Orthogneiss	LAM2	1,0	1,0	1,0	462	45,770	8,500
VR21	SR	Orthogneiss	LAM2	1,9	1,2	1,6	895	45,980	8,538
VR23	SA	Orthogneiss	LAM2	1,5	2,0	1,2	978	45,970	8,574
VR24	SA	Orthogneiss	LAM2	1,9	2,0	1,0	961	45,970	8,573
VR26	AN	Orthogneiss	LAM2	2,0	1,2	1,6	987	46,000	8,628
VR31	AN	Orthogneiss	LAM2	3,0	2,2	3,5	683	45,800	8,505
VR32	SA	Orthogneiss	LAM2	1,6	1,2	1,3	670	45,799	8,504
VR46	AN	Orthogneiss	LAM2	8,0	3,0	3,0	754	45,833	8,510
VR09	SR	Orthogneiss	LPN	1,5	1,0	1,0	684	45,827	8,526
VR25	AN	Orthogneiss	LPN	3,5	3,5	2,0	1018	46,000	8,627
VR38	SA	Orthogneiss	LPN	4,0	1,7	2,5	825	45,942	8,710
VR40	AN	Orthogneiss	LPN	2,3	2,0	1,5	875	45,915	8,642
VR41	SR	Orthogneiss	LPN	1,0	1,9	1,5	535	45,904	8,770
VR49	SR	Orthogneiss	LPN	1,7	1,5	1,1	640	45,858	8,721
VR50	SR	Orthogneiss	LPN	2,5	2,0	1,6	628	45,861	8,717
VR54	SA	Orthogneiss	LPN	2,6	1,5	1,2	790	45,872	8,722
ER36	SA	Orthogneiss	LPN	1,6	1,6	1,2	941	46,010	8,642
ER133	SR	Orthogneiss	LPN	1,6	1,0	1,6	704	45,919	8,741
ER167	AN	Orthogneiss	LPN	4,0	3,0	2,0	791	45,872	8,722
ER184	AN	Orthogneiss	LPN	1,8	2,0	2,0	354	45,707	8,534
ER185	AN	Orthogneiss	LPN	1,5	1,0	0,5	353	45,706	8,535
ER187	AN	Paragneiss	LPN	2,5	2,8	0,6	326	45,706	8,532
ER190	AN	Orthogneiss	LPN	-	-	-	697	45,866	8,719
GUER01	SA	Orthogneiss	LPN	5,0	4,0	4,0	848	46,279	9,020
GUER02	SA	Orthogneiss	LPN	2,4	4,0	1,8	840	46,278	9,021
PARU01	AN	Orthogneiss	LPN	3,3	3,2	2,9	1253	46,241	9,054
ME129	SA	Orthogneiss	LPN	-	-	-	402	45,825	8,894
ME131	SA	Orthogneiss	LPN	1,0	0,6	1,6	441	45,834	8,950
ME134	SR	Orthogneiss	LPN	0,6	0,6	0,6	459	45,832	8,969
ME135	SA	Orthogneiss	LPN	1,3	0,5	1,3	411	45,816	8,935
ER188	SR	Rhyolite	LV	-	-	-	542	45,869	8,702
ER193	SR	Rhyolite	LV	-	-	-	390	45,774	8,740
VR27	SR	Orthogneiss	MR1	1,8	1,2	1,0	811	45,847	8,506
Briallo 34	SA	Orthogneiss	MR3	-	-	-	518	45,777	8,379
Briallo 6	AN	Orthogneiss	MR3	4,0	3,0	1,0	516	45,777	8,379
Briallo 7	SR	Orthogneiss	MR3	1,3	0,9	0,6	503	45,775	8,381
Bugnate 18	AN	Orthogneiss	MR3	5,0	5,5	3,0	520	45,754	8,395
Curlera 35	SR	Orthogneiss	MR3	2,0	3,0	0,9	442	45,769	8,387
Hitsch 99	SR	Orthogneiss	MR3	2,5	2,5	1,0	399	45,757	8,421
ME20	SR	Calcarenite	PMC	-	-	-	373	45,846	8,953
ME21	SR	Calcarenite	PMC	-	-	-	373	45,846	8,952
ME23	SR	Calcarenite	PMC	-	-	-	391	45,846	8,950
ME24	SR	Calcarenite	PMC	-	-	-	373	45,846	8,953
ME29	SR	Calcarenite	PMC	-	-	-	345	45,847	8,950
ME271	SR	Calcarenite	PMC	-	-	-	386	45,845	8,951
ME273	SR	Calcarenite	PMC	-	-	-	373	45,846	8,952
ME274	SR	Conglomerate	PMC	-	-	-	367	45,838	8,934
ME275	SR	Conglomerate	PMC	-	-	-	415	45,835	8,919
ME276	SR	Breccia	PMC	2,6	2,6	3,3	324	45,831	8,881
VR05	AN	Paragneiss	SL	2,5	1,0	1,2	682	45,799	8,503
VR13	SA	Chloritoid micaschist	SL	5,0	2,0	1,4	760	45,843	8,509
ER127	SA	Garnet micaschist	SL	1,7	1,7	1,4	608	45,796	8,502
Bugnate 36	AN	Garnet gneiss	SL	5,0	3,0	2,0	507	45,754	8,401
Colma 20	AN	Garnet micaschist	SL	2,0	1,5	2,0	556	45,835	8,376
Colma 21	SA	Garnet micaschist	SL	3,0	2,5	1,0	530	45,836	8,377
Colma 22	SA	Garnet micaschist	SL	4,0	2,0	2,5	500	45,839	8,379
Curlera 12	SR	Kinzigite	SL	1,6	1,4	0,9	445	45,769	8,381
Grassona 25	AN	Micaschist	SL	8,0	6,0	2,5	519	45,818	8,370
Grassona 31	SR	Garnet micaschist	SL	3,4	2,0	1,0	543	45,816	8,371
Buccone 37	SR	Quartzite	ZC	1,0	0,8	0,5	417	45,766	8,434

Unit label	Geologic unit	Geographic distribution	Petrography	Erratic boulders
IVK	Ivrea-Verbano	Lower Ossola Valley, right inner slope of Lake Maggiore	Granulites, garnet, biotite, plagioclase, quartz and sillimanite metapelites	Puffer 11, Grassona 24, Egro 28, VR06, VR20, ER01, ER186
LAM1	Serie dei Laghi (Basement)	Lower Ossola Valley, Orta Valley, Lake Maggiore slopes downstream Brissago (right) and Bellinzona (left)	Garnet, biotite, plagioclase, quartz, sillimanite and muscovite paragneiss and micaschists	VR15, VR16, VR17, VR18, VR37, VR39, VR48
LAM2		Lake Maggiore slopes downstream Brissago (right) and Bellinzona (left)	Quartz, feldspars, green biotite, allanite, ilmenite, rare garnet. Orthogneiss with myrmekite	VR03, VR21, VR23, VR24, VR26, VR31, VR32, VR46
PMC	Serie dei Laghi (Sedimentary Cover)	Velmaio (Bévera Valley), Gaggiolo and Laveggio valleys (Mendrisio District), Lanza Valley (Varese Province)	Clast-supported polygenic breccia ("Invorio Breccia") composed by Permian volcanic fragments and Triassic dolostones. Clast- and matrix-supported conglomerate composed by Moltrasio limestone and Triassic dolostone ("Prella Conglomerate"), bioclastic calcirudites and calcarenites ("Ternate Formation").	ME20, ME21, ME23, ME24, ME29, ME271, ME273, ME274, ME275, ME276
GLA	Graniti dei Laghi	Lower Ossola Valley	Granite, granodiorite	Antenna 1, Briallo 33, Carcegna 50, VR14, VR19, VR28, VR29, VR30, VR42, VR43, VR44, VR45, VR47, ME130
BG	Bergell batholit	Bellinzona area	Granodiorite, tonalite	GUDO01, ER191
LV	Lugano volcanite	Valcuvia Valley	Rhyolite	ER188, ER193
ZC	Canavese Zone	Lower Ossola Valley	Gneiss, schists, Permian diorite, serpentinites, and sedimentary carbonate and siliceous rocks.	Buccone 37
SL	Sesia-Lanzo Zone	Lower Ossola Valley and Anzasca Valley	Albite, white mica orthogneisses and schists; jadeite pyroxene, garnet micaschists; omphacite pyroxene, glaucophane ± chloritoid eclogites and glaucophanites.	Curlera 12, Colma 20, Colma 21, Colma 22, Grassona 25, Grassona 31, Bugnate 36, VR05, VR13, ER127
MR1	Monte Rosa	Anzasca Valley, middle Ossola Valley	Albite, quartz, white mica, chlorite and garnet fine-grained gneiss; chloritoid, phengite, garnet ± kyanite, talc, chlorite micaschists.	VR27
MR3			K-feldspar megacrysts metagranitoids.	Briallo 6, Briallo 7, Bugnate 18, Briallo 34, Curlera 35, Hitsch 99
ADMG	Adula and Maggia nappes	Mesolcina Valley, Blenio Valley, Riviera Valley, Verzasca Valley, Maggia Valley	Paragneiss and micaschists with quartz, feldspars, biotite, minor white mica and garnet, tourmaline and apatite.	VR53, VR55, ER132
AON	Antrona Zone	Antrona and Anzasca Valleys	Garnet, glaucophane and omphacite clinopyroxene metabasites; serpentinites.	Bugnate 17, Briallo 32, VR02, VR04, VR22, VR33, VR51, VR52, ER192
MO-CAM-BEL	Moncucco-Orselina Camughera	Middle Ossola Valley	Biotite, white mica, garnet and staurolite paragneiss, micaschists and metagranitoids; graphitic schists; basic metavolcanites.	Buccone 38, Armeno 39
LPN	Lower Penninic nappes (Monte Leone, Lebendun, Simano, Antigorio, Leventina and Verampio)	Upper Ossola Valley, inner Ticino (including Maggia and Verzasca) valleys	Quartz, feldspars, red to brown biotite, ilmenite, minor white mica. Orthogneiss with occurrence of myrmekite.	PARU01, GUER01, GUER02, VR09, VR25, VR38, VR40, VR41, VR49, VR50, VR54, ER36, ER133, ER167, ER184, ER185, ER187, ER190, ME129, ME131, ME134, ME135
HN	Gotthard Massif	Leventina and Blenio valleys	Biotite, white mica, ± garnet micaschists. Metagranite	VR36

Tab. 2 - Overview of the geological units of the Ticino-Toce catchment and the provenance of the studied erratic boulders.

2012) or used as holy sites (e.g. Prea Guzza). Within the Orta and Verbano morainic amphitheaters, big boulders are not limited to the last glaciation, but were also found external to the LGM frontal moraines (Braakhekke et al., 2020; Kamleitner et al., 2022a).

3. MATERIALS AND METHODS

In the present work, provenance analysis was applied to erratic boulders found in the Orta, Verbano, and Ceresio end moraine systems (Fig. 1). The respective boulders were located during field campaigns related to different mapping and dating projects (Bernoulli et al., 2017, 2018; Braakhekke et al., 2020; Kamleitner et al., 2022a). In total more than 500 erratic boulders were considered, out of which 105 boulders were chosen for provenance studies as their source rocks were well recognized (Tab. 1). Erratic boulders were grouped by their source rock on the base of the simplified geological map of the catchments, which derives from Bigi et al. (1983), swisstopo (2005) and Piana et al. (2017).

More than 260 erratic boulders were located in the lower Ticino and Orta valleys, geographically positioned in a GIS database and described in size and roundness type (Tab. 1). Most of the erratics are related to frontal or lateral moraine ridges but boulders situated on bedrock close to the trimline are also included (Fig. 1). The size of the boulders varies from 1 m^3 minimum to >300 m^3 max (Tab. 1, Fig. 4). The exposure age of 54 erratic boulders was defined with cosmogenic nuclide exposure dating (Braakhekke et al., 2020; Kamleitner et al., 2022a). Out of these, 19 boulders are related to the maximum advances and 31 located in the withdrawal moraines or in the valley floor. Four boulders from the Verbano end moraine system were dated to pre-LGM ice advance(s) (VR19, VR42, VR30 and VR45). Four more boulders (GUDO01, GUER01, GUER02, PARU01) come from the Lateglacial deposits in Ticino Valley. These eight boulders are included in Table 1 but not considered in the discussion. A description of the boulder petrography was provided in the field. For 85 boulders (including exposure dated and other selected erratics), thin section analysis was performed in order to recognize the metamorphic facies of gneiss and micaschist lithotypes (Fig. 5).

An overall 289 erratic boulders related to the Ceresio morainic amphitheatre were mapped and inventoried in a GIS geodatabase during Quaternary geological cartography for the Sheet 152 Mendrisio-Como of the Swiss Geological Atlas 1:25,000 (see Bernoulli et al., 2017, 2018). 101 erratic boulders were considered as deposited during pre-LGM glacial advances, whereas 188 boulders are located within limits of the LGM expansion in the geological map (Bernoulli et al., 2017). The eleven boulders included in the present work were lithologically recognized (Tabs. 1 and 2) and, even if outside the mapped LGM (Bini et al., 2014; Bernoulli et al., 2017), they yield information about the flowline of this branch of the glacier.

3.1. Provenance of the boulders

The provenance of more than hundred erratic boulders related to the LGM of the Orta, Verbano, and Cere-

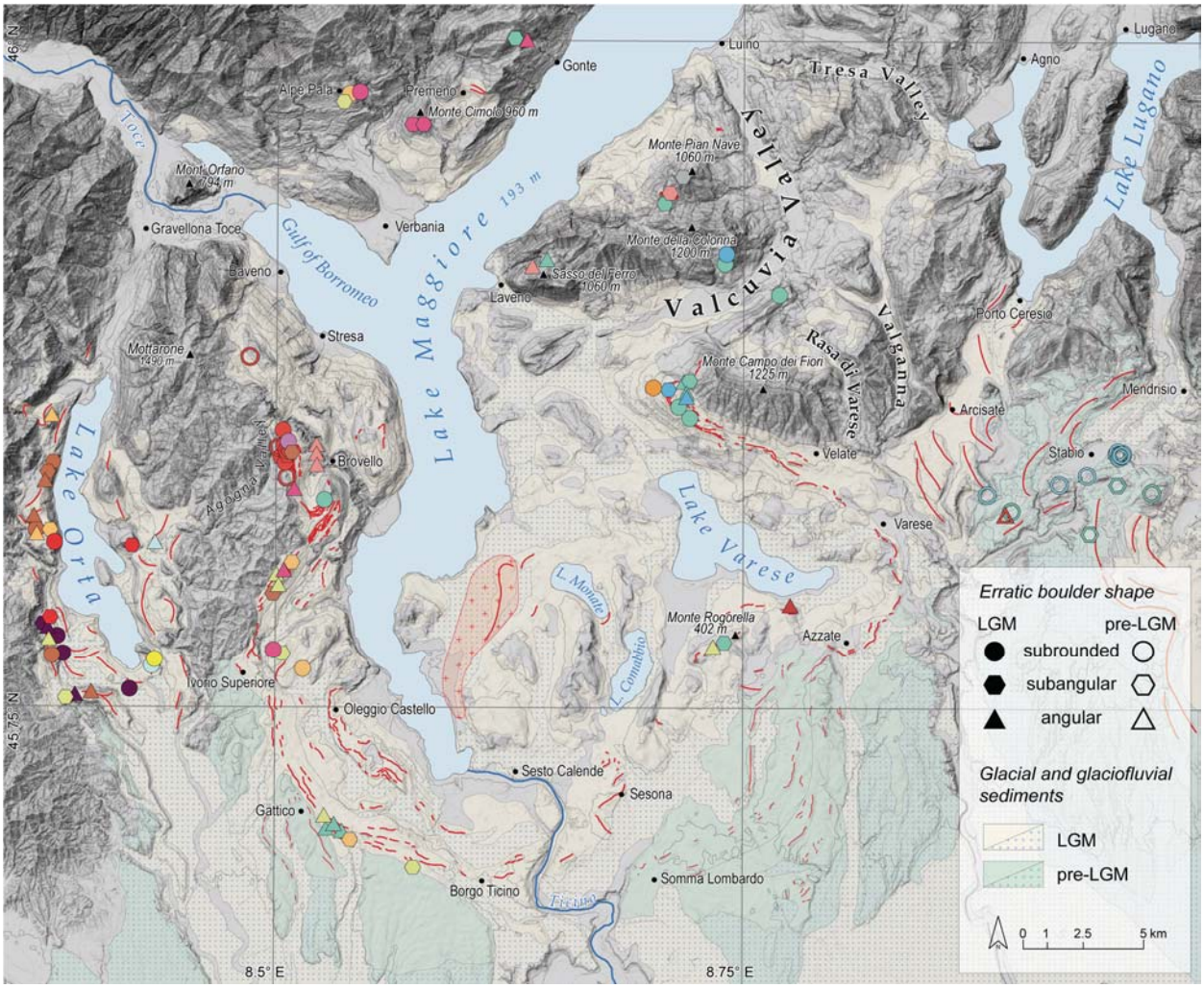

Fig. 6 - Distribution and lithology of the studied erratic boulders in the Orta-Verbano and Ceresio morainic amphitheaters. For color codes see legend of Fig. 2. Red crosses indicate areas where Baveno granite boulders (GLA unit) were recognized during railway constructions in the 19th century (Omboni, 1861; Gentilli, 1866; Salmojraghi, 1882). Mapped moraine ridges (Bini et al., 2014; Braakhekke et al., 2020; Kamleitner et al., 2022a) are shown as red lines. Distribution of glaciofluvial and glacial sediments was modified from the geological maps of Piedmont (1:250,000; Piana et al., 2017) and Lombardy (1:250,000; Montrasio et al., 1990) and the Swiss Geological Atlas 1:25,000 (Bernoulli et al., 2017, 2018).

sio glacier lobes, was identified using thin section analysis (85 samples) and visual interpretation in the field (30). The petrographic characteristics of the boulders are reported in Table 2 and illustrated in Fig. 6. Boulders show petrographic provenance clustering in the wide area covered by the Ticino and Toce glacier snouts. An overall 48 samples are related to bedrock units located south of the Insubric Line, the sector closest to the glacier termini. The most frequently encountered lithologies are those related to the Southalpine metamorphic basement (IVK and LAM, with three boulders in the Orta and 19 in the Verbano system, respectively), the Permian granites (GLA, with three boulders in Orta, ten in the Verbano system, and one erratic in the Ceresio end moraines, respectively) and the Lugano Volcanites (LV, two erratics in the Verbano end moraine system). The occurrence of GLA erratics was also documented in till north of Sesto Calende (Omboni, 1861; Salmojraghi, 1882). Erratic boulders from the Sesia-Lanzo Zone (SL) build a second important petrographic group, particularly in the Orta end moraine system (seven boulders in the Orta Valley and three in the Verbano system, respectively). MR and MO-CAM-BEL units are well represented in the Orta system (eight samples), while one boulder (VR27, Fig. 5H) was collected in the Verbano area. Ophiolitic boulders (Antrona Zone, AON) are present in both Orta and Verbano amphitheatres with two and seven samples, respectively. In the Verbano end moraine system, erratics sourced from the Antrona Zone are widely scattered. AON erratics were found associated with lateral moraine deposits north of Verbania (Fig. 4E) and along the western margin of the former Verbano lobe. Three boulders sampled from Verbano frontal moraines show AON signature. One of them (ER192) is located

just south of Lake Varese. Lower Penninic boulders (LPN) are lacking in the Orta amphitheatre while 15 and four LPN samples were collected in the Verbano and Ceresio end moraine systems, respectively. Finally, one boulder of the Helvetic Gotthard Massif was collected from Monte Pian Nave (VR36; Fig. 6), while one granodioritic boulder, coming from the Bergell batholith (BG), was found south of Lake Varese. In the Ceresio sector most of the boulders belong to the Southalpine sedimentary covers (Tab. 1, Fig. 4F); because no local valley glaciers could have developed in the low-elevation sector, these boulders were transported by glacier diffluence. Boulder lithologies indicate that both the Ticino and the Adda branches could have been responsible for erratic transport.

As expected from the scarce mixing of the supraglacial fluxes, the distribution of analyzed erratic boulders shows an inhomogeneous lithological distribution. The lithotypes from bedrock of the Ossola Valley (AON, MR, IVK, SL) are largely distributed in the Orta lobe and on the western side of the Verbano lobe. Nevertheless, erratics sourced from Ossola Valley were also found in the central part of the end moraine system, south of Lake Varese. On the other hand, lithotypes of BG, ADMG and HN, originating from the Ticino Valley network as well as Lugano Volcanites (LV) were found only in the very left sector of the Verbano end moraine system. In contrast, the Lower Penninic bedrock (LPN) characterizes the upper catchments of Ticino and Toce glaciers. Occurrence of Penninic erratic boulders is common across the Verbano lateral-frontal moraine complex.

Roundness of erratic boulders varies from angular to sub-rounded (Tab. 1). Most of the angular boulders are located on the outermost frontal and lateral moraines, while those located on internal moraines are mostly sub-angular to sub-rounded. An exception is represented by GLA boulders that, despite their position, are mostly sub-rounded (Fig.4C). This can be ascribed to the particular surficial exfoliation (Ollier, 1967) of granite bedrock on the slopes of the Mottarone (Fig. 6) and the subsequent shaping during the transportation, even if from short distance.

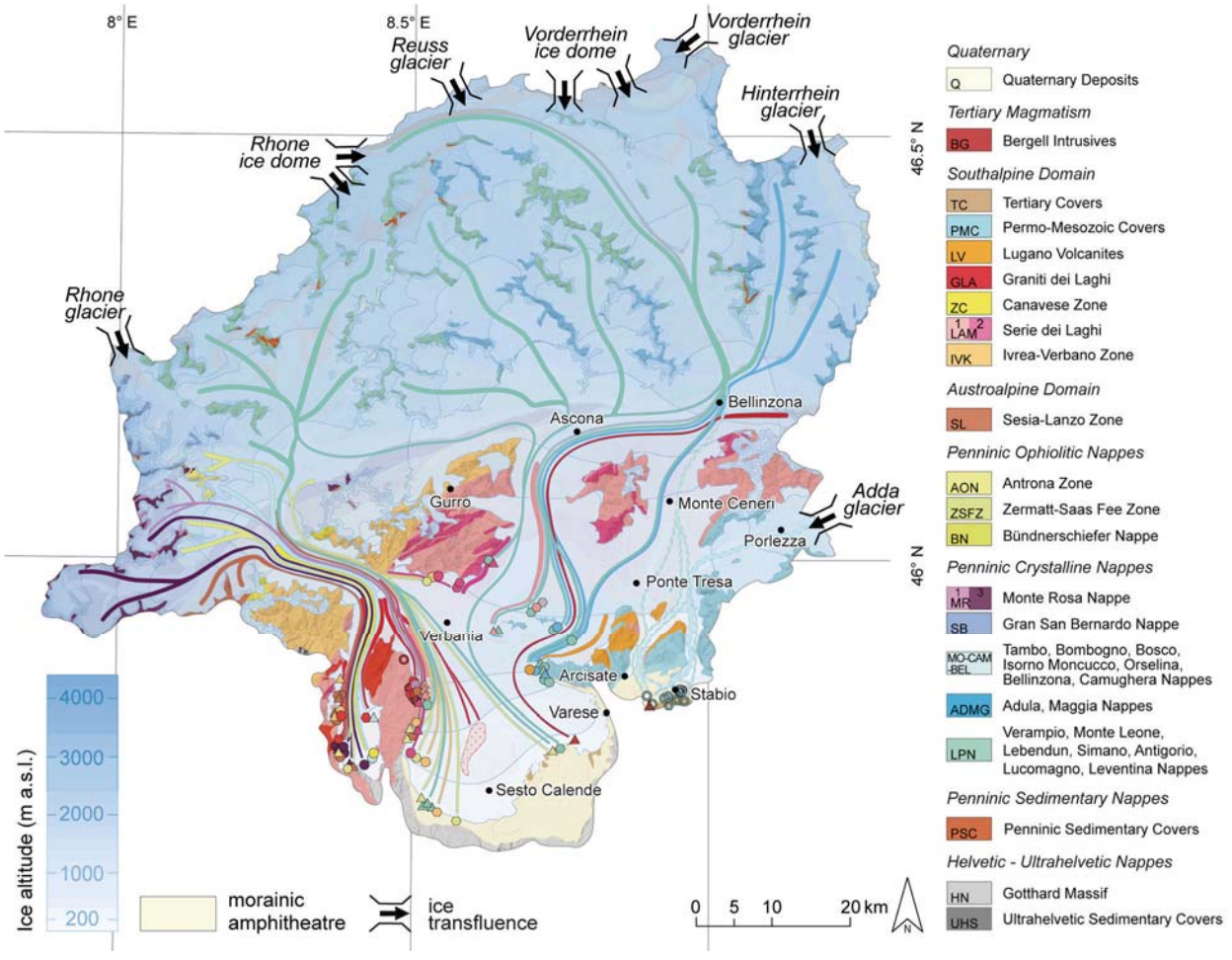

Fig. 7 - Flowlines of the Ticino-Toce glacier system (extent modified after Bini et al. 2009, Braakhekke et al., 2020, Kamleitner et al., 2022a) during the LGM inferred from erratic boulder lithologies. Dashed trajectories in the Ceresio lobe are suggested by boulders located outside the pre-LGM limit (Bini et al., 2014; Bernoulli et al., 2017; no dates available). For symbols see legend of Figure 6.

4. DISCUSSION

4.1. Inferred ice flow paths in the Ticino-Toce system

The distribution of index erratics within the Orta, Verbano, and Ceresio end moraine systems found in this study can be coupled with observations made by early authors. The lithological provenance of granite and gneiss erratic boulders that have been subsequently removed by anthropogenic quarrying activities is reported by CAI (1914). It is remarkable that Omboni (1861) already noticed that the moraines west of Lake Maggiore are dominated by boulders of the Toce catchment, while those close to the Campo dei Fiori slope (opposite, eastern side) are characterized by boulders of the inner Ticino basement. Baveno granite boulders (GLA) are common in the lateral moraines (Fig. 4B) of the western part of the Verbano end moraine system deposited by the Toce glacial branch at this point welded with the Ticino glacier. However, Baveno granite boulders, as well as the presence of this type of rock in lodgment till, were recognized in early excavations for the construction of a railway line between Sesto Calende and Lake Varese in the 19th Century (i.e. in the eastern frontal sector of the Verbano system; Fig. 6; Omboni, 1861; Gentilli, 1866; Salmojraghi, 1882).

Petrological investigations undertaken in this study and from the literature (Omboni, 1861; Gentilli, 1866; Salmojraghi, 1882; CAI, 1914) combined with exposure dating of selected erratic boulders and geomorphological analysis of earlier work (Braakhekke et al., 2020; Kamleitner et al., 2022a) yield crucial insights into glacier flow paths of the Ticino-Toce glacier during the LGM (Fig. 7). Boulder lithologies originating from the Ossola Valley indicate that the LGM Orta morainic amphitheatre and the western section of the LGM Verbano end moraine system correspond to the flow of the Toce glacier. Most of the boulders belong to the southalpine basement (IVK and LAM), the Permian batholith (GLA), the SL and MR Alpine nappes and the ophiolites (AON). It is remarkable that the inner sector of the Toce catchment is scarcely represented in the Orta moraines (Braakhekke et al. 2020), whereas boulders of the LPN are common in the western frontal moraines of Verbano (Fig. 6), indicating a significant persistence of the dispersal train. Boulders transported by the Toce glacier are widely found on LGM lateral and frontal moraines of the Verbano amphitheatre, including the sector south of Lake Varese. This suggests a dominance of the Toce glacier over the Ticino glacier. Ticino glacier may have hence been confined to the eastern flank of the system (Fig. 7). The Toce system is characterized by a shorter stream course while at the same time being notably steep with accumulation areas reaching above 4000 m a.s.l. In comparison, the Ticino catchment is more than two-and-a-half times the size of the Toce basin, yet mountain peaks are lower, the slopes are gentler, and the thalweg is longer (Fig. 3). An important divergence of the Toce glacier was located along the Vigezzo Valley draining ice towards Ticino Valley and into high Canobbina Valley, as testified by glacigenic deposits (Boriani & Burlini, 1995); again this indicates the predominance of the Toce glacier. These thoughts agree well with the palaeoglacier model by Seguinot et al. (2018), which shows that the Ticino glacier likely reached the mountain front slightly later, where it faced the physical obstacle of the spreading Toce piedmont glacial lobe. Likely due to ice congestion, flow of the Ticino glacier was forced to diverge to the east-southeast across Monte Ceneri Pass and to occupy the Vedeggio and Cassarate valleys (Fig. 2). In the Ceresio sector, it merged with the branch of the Adda glacier system, coming through Porlezza Valley (Bini, 1997; Castelletti et al., 2014). The abundance of sedimentary rock boulders indicates that the Ticino glacier eroded the sedimentary covers of the area and then formed the main part of the western Ceresio lobe ending at Arcisate. Probably it made also a part of the eastern Ceresio lobe, ending at Stabio where it merged with the western part of the Adda glacier system (Bini, 1997; Scapozza et al., 2014; Bernoulli et al., 2018). In the lower reaches of Ticino Valley, a second divergence at Luino may have promoted ice exchange between Valcuvia Valley and Tresa Valley.

According to the distribution of erratic boulder lithologies in the Orta, Verbano, and Ceresio end moraine systems, the major LGM ice streams of Ticino and Toce glaciers are suggested to have been as follows (Fig. 7):

- the LGM Orta glacier lobe was mainly fed by the Anzasca tributary glacier (Braakhekke et al., 2020) with a contribution of ice from the Ossola/Toce valley glacier in the eastern parts of the lobe.
- ice from the Toce valley glacier built up the western sector of the LGM Verbano glacier lobe and possibly extended far towards the southeast, at least during the early phase of the LGM.
- the Ticino glacier dominated the eastern flank of the Verbano system, in the Lake Varese and Campo dei Fiori sectors.
- through a diffluence across Monte Ceneri Pass, Ticino glacier fed western parts of the Ceresio lobe between Porto Ceresio and Arcisate.

4.2. Implications for Ticino-Toce glacier dynamics

The complex dynamics of the Ticino-Toce glacier network were strongly influenced by the asymmetry of the mountain catchments. A key role was played by the highest sector of the Toce accumulation area represented by the high Monte Rosa - Fletschorn ridgeline, running over 3000 m a.s.l. with peaks over 4000 m a.s.l. The rapid spread of the Toce catchment glaciers, taking into account the short travel distances (~100 km of the Toce against ~150 km max of the Ticino Leventina, Fig. 3), promoted early arrival of the Toce glacier in the piedmont area. The possibly rapid response of the Toce catchment to climate changes of MIS 3 and the onset of the LGM supports the marked spread of Toce ice over a large sector of the Verbano piedmont lobe. Presumably, the larger but slower Ticino glacier was pushed to the east and forced to spread in the prealpine area of the Lake Lugano region. These results yield interesting implications for the reconstruction of the evolution and interconnections of large glaciated networks in mountain ranges. The fastest glaciers might have played a role in blocking the flow of glaciers with greater inertia and forced transfluences/diffluences if topography allowed

for it.

During the LGM, the Alps were covered by a network of interconnected valley glaciers (Ivy-Ochs et al., 2022). Hence, many glacier systems were affected by merging trunk glaciers. The presented data from Toce and Ticino catchments underlines how the reaction time of neighboring glacier systems may vary due to inherent differences in catchment geometry, especially when the accumulation areas show a strong asymmetry. A similar behavior of ice overflowing into previously non-glaciated valleys forced due to blockage by another glacier was reported for trunk glaciers in the lower Inn and Salzach valleys (van Husen, 2004; Reitner et al., 2010), but can be conceivable in other sectors of the Alps and in other mountain ranges as well.

In addition, palaeoclimatic models suggest that precipitation was irregularly distributed in time and space across the Alps contributing to anomalous ice accumulation throughout the LGM time bracket (Kuhlemann et al., 2008; Luetscher et al., 2015; Del Gobbo et al., 2022). Moreover, the different distribution of major ice-flows can be related to how the accumulation areas, and specifically the major ice-domes, reacted to the climate change promoting the spread of the glaciers. According to modelling studies on the Isere, Rhone, and Rhine paleoglaciers (Coutterrand, 2010; Jouvet et al., 2017; Cohen et al., 2018), the contribution from different sectors of an accumulation area can be traced from the highest parts to the outlet. Glacier simulations further suggest increased basal erosion underneath confluencing ice streams (Cohen et al., 2018; Jouvet et al., 2021). Some valley reaches of the Rhine catchment were characterized by very slow advance (Cohen et al., 2018), and this characteristic may be inferred for the advance of the Ticino glacier through the valley section south of Bellinzona, which is up to 4.5 km wide with a very low gradient. The model of Seguinot et al. (2018) shows that the Toce glacier extended to Gravellona Toce several times already in the MIS 4 and MIS 3 cold phases and may have molded the valley outlet. On the other hand, the Ticino glacier arrived in the Lake Maggiore area only during the LGM (Seguinot et al., 2018), when the paleoclimatic conditions (Del Gobbo et al., 2022) allowed the spread of a large glacier and its persistence until the final collapse at about 18 ka (Wirsig et al., 2016; Ivy-Ochs et al., 2022). Moreover, the shallow elevation in the lower Toce Valley bottom and in the Gulf of Borromeo is in contrast to the deep trough of Lake Maggiore (Cazzini et al., 2020) and may indicate a more effective subglacial carving by the Ticino glacier. This may suggest that the Toce glacier prevailed at the LGM onset and the Ticino glacier at the LGM climax.

5. CONCLUSIONS

The study of the provenance of erratic boulders of the Ticino-Toce glacier system provides interesting insights into the development of a large LGM glacial network and its outflow in the prealpine and piedmont areas. The distribution of erratic boulders shows a dominance of the Toce glacier in the Orta lobe and in the western-central sector of the Verbano lobe. The LGM Orta lobe was predominantly fed by ice from Anzasca Valley, a right tributary glacier of the Toce valley glacier. Despite the much larger catchment, lithologies indicative of the Ticino glacier are largely limited to the eastern sector of the LGM Verbano lobe and the western parts of the Ceresio system, where Ticino ice merged with the westernmost branch of the Adda glacier system. The topographic differences in the overall accumulation areas, with maximum elevations (>4000 m a.s.l.) and steep slopes in the Toce catchment, promoted the sudden and rapid spread of the Toce glacier, whose path was shorter (<100 km) in comparison to the Ticino glacier (around 150 km). The early arrival of Toce glacier possibly resulted in the damming of the Ticino glacier and fostered the diffluence of Ticino ice into the prealpine area to the east, merging with the western branch of the Adda glacier, where elevations were too low for hosting independent valley glaciers during the LGM.

The dynamics of the two studied LGM glaciers highlight the importance of topography as a driver for ice build-up and development of valley glaciers. Faster glaciers may force slower trunk glaciers to a different path. Considering the topographic setting of the Alpine area this could have been a common phenomenon also in past glaciations. The provenance of boulders can thus provide an important tool for determining glacier flow trajectories that could have been affected by unequal glacier evolution.

ACKNOWLEDGMENTS

Funding by the Swiss National Science Foundation is gratefully acknowledged [SNF grant number 175794, 2017]. The reviews provided by two anonymous reviewers greatly improved our manuscript. We also thank A. Fontana (A.E.) for his comments.

REFERENCES

Baudin T., Marquer D., Persoz F. (1993) - Basement-cover relationships in the Tambo Nappe (Central Alps, Switzerland); geometry, structure and kinematics. The Geometry of Naturally Deformed Rocks, vol. 15 (3-5). Pergamon, Oxford, 543- 553.

Becker P., Seguinot J., Jouvet G., Funk M. (2016) - Last Glacial Maximum precipitation pattern in the Alps inferred from glacier modelling. Geographica Helvetica, 71, 173-187.

Berger A., Schmid S.M., Engi M., Bousquet R., Wiederkehr M. (2011) - Mechanisms of mass and heat transport during Barrovian metamorphism: A discussion based on field evidence from the Central Alps (Switzerland/northern Italy). Tectonics, 30, 1-17.

Bernoulli D., Ambrosi C., Scapozza C., Castelletti C., Wiedenmayer F. (2017) - Foglio 1373 Mendrisio (parte Est) con parte Ovest del foglio Como. Atlante geologico della Svizzera 1:25000, Carta 152.

Bernoulli D., Ambrosi C., Scapozza C., Stockar R. Schenker F. L., Gaggero L., Antognini M., Bronzini S. (2018) - Foglio 1373 Mendrisio (parte Est) con parte Ovest del Foglio Como. Atlante geologico della Svizzera 1:25000, Note esplicative 152. data.geo.admin.ch/ch.swisstopo.geologie-geologischer_atlas/erlaeuterungen/GA25-ERL-

152.pdf
Bertotti G., Picotti V., Bernoulli D., Castellarin A. (1993) - From rifting to drifting: Tectonic evolution of the South-Alpine upper crust from the Triassic to the Early Cretaceous. Sedimentary Geology, 86, 53-76.
Bigi G., Castellarin A., Coli M., Dal Piaz G.V., Sartori R., Scandone P., Vai G.B. (1983) - Structural Model of Italy. Scale 1:500.000. C.N.R., Progetto Finalizzato Geodinamica. SELCA, Firenze.
Bigioggero B., Boriani A., Colombo A., Tunesi A. (1981) - Età e caratteri petrochimici degli ortogneiss della zona Moncucco-Orselina nell'area Ossolana. Rendiconti Società Italiana di Mineralogia e Petrografia, 38, 207-218.
Bini A. (1997) - Stratigraphy, chronology and paleogeography of Quaternary deposits of the area between the Ticino and Olona rivers (Italy-Switzerland). Geologia Insubrica, 2, 21-46.
Bini A., Cita M.B., Gaetani M. (1978) - Southern Alpine lakes - Hypothesis of an erosional origin related to the Messinian entrenchment. Marine Geology, 27, 271-288.
Bini A., Buoncristiani J.F., Couterrand S., Ellwanger D., Felber M., Florineth D., Graf H.R., Keller O., Kelly M., Schlüchter C., Schoeneich P. (2009) - Die Schweiz während des letzteiszeitlichen Maximums (LGM). Bundesamt für Landestopografie swisstopo, Wabern.
Bini A., Bussolini C., Turri S., Zuccoli L. (2014) - Carta geologica alla scala 1:100.000 dell'anfiteatro morenico del Verbano. Sibrium, 28, 25-77.
Boriani A., Burlini L., Sacchi R. (1990a) - The Cossato-Mergozzo-Brissago Line and the Pogallo Line (Southern Alps, Northern Italy) and their relationships with the late-Hercynian magmatic and metamorphic events. Tectonophysics, 182, 91-102.
Boriani A., Giobbi Origoni E., Borghi A., Caironi V. (1990b) - The evolution of the "Serie dei Laghi" (Strona-Ceneri and Scisti del Laghi): the upper component of the Ivrea-Verbano crustal section; Southern Alps, North Italy and Ticino, Switzerland. Tectonophysics, 182, 103-118.
Boriani A., Burlini L. (1995) - Carta geologica della Valle Cannobina. Dipartimento di Scienze della Terra dell'Università degli Studi di Milano, Milano.
Braakhekke J., Ivy-Ochs S., Monegato G., Gianotti F., Martin S., Casale S., Christl M. (2020) - Timing and flow pattern of the Orta Glacier (European Alps) during the Last Glacial Maximum. Boreas, 49, 315-332.
CAI (1914) - I massi erratici nella regione dei tre laghi. Premiata Tip. Succ. Fratelli Fusi, Pavia.
Castelletti L., Livio F., Martinelli E., Michetti A.M., Motella De Carlo S. (2013) - Recenti ricerche paleoecologiche in ambito lariano svolte in collaborazione fra Università dell'Insubria e Laboratorio di archeobiologia dei Musei Civici di Como. Rivista archeologica dell'antica Provincia e Diocesi di Como, 195, 115-128.
Cazzini F.F., Amadori C., Bosino A., Fantoni R. (2020) - New seismic evidence of the Messinian paleomorphology beneath Lake Maggiore area (Italy). Italian Journal of Geosciences, 139, 195-211.
Compagnoni R., Dal Piaz G.V., Hunziker J.C., Gosso G., Lombardo B., Williams P.F. (1977) Rendiconti della Società Geologica Italiana di Mineralogia e Petrologia, 33, 281-334.
Coutterand S. (2010) - Etude géomorphologique des flux glaciaires dans les Alpes nord-occidentales au Pléistocène récent: du maximum de la dernière glaciation aux premières étapes de la déglaciation, PhD thesis, Université de Savoie, Savoie.
Coutterand S., Schoeneich P., Nicoud G. (2009) - Le Lobe Glaciaire Lyonnais au maximum würmien glacier du Rhône ou/et glaciers savoyards? In Deline P., Ravanel L. (eds.): Neige et glace de Montagne. Reconstitution, Dynamique, Pratiques, 11-22. Collection EDYTEM, Cahiers de Géographie, Le Bourget-du-Lac Cedex.
Cohen D., Gillet-Chaulet F., Haeberli W., Machguth H., Fischer U.H. (2018) - Numerical reconstructions of the flow and basal conditions of the Rhine glacier, European Central Alps, at the Last Glacial Maximum. Cryosphere, 12, 2515-2544.
Colombi A., Pfeifer H.R. (1986) - Ferrogabbroic and basaltic meta-eclogites from the Antrona mafic-ultramafic complex and the Centovalli-Locarno region (Italy and southern Switzerland)- First results. Schweizerische mineralogische und petrographische Mitteilungen, 66: 99-11
Cummings D.I., Russell H.A.J. (2018) - Glacial dispersal trains in North America. Journal of Maps, 14(2), 476-485.
Doi: 10.1080/17445647.2018.1478752
Dal Piaz G.V. (2010) - The Italian Alps: A journey across two centuries of Alpine geology, in: Beltrando, M., Peccerillo, A., Mattei, M., Conticelli, S., Doglioni, C. (Eds.), The Geology of Italy: Tectonics and Life along Plate Margins. Journal of the Virtual Explorer, 36.
Del Gobbo C., Colucci R.R., Monegato G., Žebre M., Giorgi F. (2022) - Atmosphere-cryosphere interactions at 21 ka BP in the European Alps. Climate of the Past Discussions.
Doi: 10.5194/Cp-2022-43
De Marinis R.C. (2012) - L'arte figurativa schematica nella cultura di Golasecca. Preistoria Alpina, 46, 367-369.
Evans D.J.A. (2003) - Ice-Marginal terrestrial landsystems: active temperate glacial margins. In: D.J.A. Evans (Ed.) Glacial Landsystems. Arnold, London, 12-43.
Ferrando S., Bernoulli D., Compagnoni R. (2004) - The Canavese zone (internal Western Alps): a distal margin of Adria. Schweizerische mineralogische und petrographische Mitteilungen, 84, 237-256.
Finckh P. (1978) - Are southern Alpine lakes former Messinian canyons? - Geophysical evidence for preglacial erosion in the southern Alpine lakes. Marine Geology, 27, 289-302.
Florineth D., Schlüchter C. (1998) - Reconstructing the Last Glacial Maximum (LGM) ice surface geometry and flowlines in the Central Swiss Alps. Eclogae Geologicae Helvetiae, 91, 391-407.
Frasca M., Vacha D., Chicco J., Troilo F., Bertolo D.

(2020) - Landslide on glaciers: an example from the Western Alps (Cogne- Italy). Journal of Mountain Science, 17, 1161-1171.
Doi: 10.1007/s11629-019-5629-y

Frey M., Hunziker J.C, O'Neil J.R., Schwander H.W. (1976) - Equilibrium-disequilibrium relations in the Monte Rosa granite, western Alps; petrological, Rb-Sr and stable isotope data. Contributions to Mineralogy and Petrology, 55, 147-179.

Frey M., Desmons J., Neubauer F. (1999) - The new metamorphic map of the Alps. Schweizerische mineralogische und petrographische Mitteilungen, 79, 1-4.

Gentilli A. (1866) - Sopra un fenomeno del terreno glaciale di Vergiate. Atti Società Italiana di Scienze Naturali, 9, 426-427.

Gianotti F., Forno M.G., Ivy-Ochs S., Monegato G., Pini R., Ravazzi C. (2015) - Stratigraphy of the Ivrea morainic amphitheatre (NW Italy): an updated synthesis. Alpine and Mediterranean Quaternary, 28, 29-58.

Goodsells B., Hambrey M.J., Glasser N. (2005) - Debris transport in a temperate valley glacier: Haut Glacier d'Arolla, Valais, Switzerland. Arctic, Antarctic, and Alpine Research, 37, 218-232.

Graf A., Akçar N., Ivy-Ochs S., Strasky S., Kubik P.W., Christl M., Burkhard M., Wieler R., Schlüchter C. (2015) - Multiple advances of Alpine glaciers into the Jura mountains in the northwestern Switzerland. Swiss Journal of Geosciences, 108, 225-238.

Hantke R. (1983) - Eiszeitalter die jüngste Erdgeschichte der Schweiz und ihrer Nachbargebiete. Westliche Ostalpen mit ihrem bayerischen Vorland bis zum Inn-Durchbruch und Südalpen zwischen Dolomiten und Mont Blanc. Ott Verlag, Thun.

Hunziker J.C., Zingg A. (1980) - Lower palaeozoic amphibolite to granulite facies metamorphism in the Ivrea zone (Southern Alps, Northern Italy). Schweizerische mineralogische und petrographische Mitteilungen, 60, 181-213.

Imhof M.A., Cohen D., Seguinot J., Aschwanden A., Funk M., Jouvet G. (2019) - Modelling a paleo valley glacier network using a hybrid model: an assessment with a Stokes ice flow model, Journal of Glaciology, 65, 1000-1010.
Doi: 10.1017/jog.2019.77

Ivy-Ochs S., Lucchesi S., Baggio P., Fioraso G., Gianotti F., Monegato G., Graf A., Akçar N., Christl M., Carraro F., Forno M.G., Schlüchter C. (2018) - New geomorphological and chronological constraints for glacial deposits in the Rivoli-Avigliana end-moraine system and the lower Susa Valley (Western Alps, NW Italy). Journal of Quaternary Science, 33(5), 550-562.

Ivy-Ochs S., Monegato G., Reitner J.M. (2022) - The Alps: glacial landforms from the last glacial maximum. In: Palacios, D., Hughes, P.D., Ruiz, J.M.G., de Andrés, N. (Eds.), European Glacial Landscapes: Maximum Extent of Glaciations. Elsevier, Amsterdam, 449-460.

Jouvet G., Seguinot J., Ivy-Ochs S., Funk M. (2017) - Modelling the diversion of erratic boulders by the Valais Glacier during the last glacial maximum. Journal of Glaciology, 63, 487-498.
Doi: 10.1017/jog.2017.7

Jouvet G., Cordonnier G., Kim B., Lüthi M., Vieli A., Aschwanden A. (2021) - Deep learning speeds up ice flow modelling by several orders of magnitude. Journal of Glaciology, 1-14.
Doi: 10.1017/jog.2021.120

Kamleitner S., Ivy-Ochs S., Monegato G., Gianotti F., Akçar N., Vockenhuber C., Christl M., Synal, H.A. (2022a) - The Ticino-Toce glacier system (Swiss-Italian Alps) in the framework of the Alpine Last Glacial Maximum. Quaternary Science Reviews, 279, 107400.

Kamleitner S., Ivy-Ochs S., Manatschal L., Akçar N., Christl M., Vockenhuber C., Hajdas I., Synal H.A. (2022b) - Last Glacial Maximum glacier fluctuations on the northern Alpine foreland: geomorphological and chronological reconstructions from the Rhine and Reuss glacier systems. Geomorphology.
Doi: 10.1016/j.geomorph.2022.108548

Keller L.M., Hess M., Fügenschuh B., Schmid S.M. (2005) - Structural and metamorphic evolution of the Camughera-Moncuco, Antrona and Monte Rosa units southwest of the Simplon line, Erstern Alps. Ecloagae Geologicae Helvetiae, 98, 19-49.

Kelly M.A., Buoncristiani J.F., Schlüchter C. (2004) - A reconstruction of the last glacial maximum (LGM) ice-surface geometry in the western Swiss Alps and contiguous Alpine regions in Italy and France. Eclogae Geologicae Helvetiae, 97, 57-75.

Kuhlemann J., Rohling E.J., Krumrei I., Kubik P., Ivy-Ochs S., Kucera M. (2008) - Regional synthesis of mediterranean atmospheric circulation during the last glacial maximum. Science, 321, 1338-1340.

Larson P.C., Mooers H.D. (2004) - Glacial indicator dispersal processes: a conceptual mode. Boreas, 33, 238-249.

Luetscher M., Boch R., Sodemann H., Spötl C., Cheng H., Edwards R. L., Frisia S., Hof F., Müller W. (2015) - North Atlantic storm track changes during the Last Glacial Maximum recorded by Alpine speleothems. Nature Communications, 6, 6344.
Doi: 10.1038/ncomms7344

Maxelon M., Mancktelow N.S. (2005) - Three-dimensional geometry and tectonostratigraphy of the Pennine zone, Central Alps, Switzerland and Northern Italy. Earth-Science Reviews, 71, 171-227.

Menzies J., van der Meer J.J.M., Shilts W.W. (2017) - Sublacial Processes and Sediments. In: J. Menzies, J.J.M. van der Meer (Eds.) Past Glacial Environments, pp. 105-158.

McClenaghan M.B., Bobrowsky P.T., Hall G.E, Cook S.J. (2001) - Drift Exploration in Glaciated Terrain. The Geological Society, London.

Monegato G., Ravazzi C., Donegana M., Pini R., Calderoni G., Wick L. (2007) - Evidence of a two-fold glacial advance during the last glacial maximum in the Tagliamento end moraine system (eastern Alps). Quaternary Research, 68(2), 284-302.

Doi: 10.1016/j.yqres.2007.07.002
Monegato G., Scardia G., Hajdas I., Rizzini F., Piccin A. (2017) - The Alpine LGM in the boreal ice-sheets game. Scientific Reports, 7(1), 2078.
Novarese V. (1927) - Gli apparati morenici würmiani del Lago Maggiore e del Lago d'Orta. Bollettino dell'Ufficio Geologico Italiano 8, 1-64.
Oberhänsli R., Bousquet R., Engi M., Goffé B., Gosso G., Handy M., Höck V., Koller F., Lardeaux J.M., Polino R., Rossi P., Schuster R., Schwartz S., Spalla M.I. (2004) - Metamorphic structure of the Alps. In: Explanatory note to the map "Metamorphic structure of the Alps", Commission for the Geological Map of the World, Paris.
Ollier C.D. (1967) - Spheroidal weathering, exfoliation and constant volume alteration. Zeitschrift fur Geomorphologie, 11, 103-108.
Omboni G., (1861) - I ghiacciai antichi ed il terreno erratico della Lombardia. Atti Società Italiana di Scienze Naturali, 6, 232-299.
Piana F., Fioraso G., Irace A., Mosca P., d'Atri A., Barale L., Falletti P., Monegato G., Morelli M., Tallone S., Vigna G.B. (2017) - Geology of Piemonte Region (NW Italy, Alps-Apennines junction zone). Journal of Maps, 13(2), 395-405.
Pinarelli L., Boriani A., Del Moro A. (1993) - The Pb isotopic systematics during crustal contamination of subcrustal magmas: the Hercynian magmatism in the Serie dei Laghi (Southern Alps, Italy). Lithos, 31, 51-61.
Preusser F., Reitner J.M., Schlüchter C. (2010) - Distribution, geometry, age and origin of overdeepened valleys and basins in the Alps and their foreland. Swiss Journal of Geosciences, 103, 407-426.
Reber R., Akçar N., Ivy-Ochs S., Tikhomirov D., Burkhalter R., Zahno C., Lüthold A., Kubik P.W., Vockenhuber C., Schlüchter C. (2014) - Timing of retreat of the Reuss glacier (Switzerland) at the end of the last glacial maximum. Swiss Journal of Geosciences, 107, 293-307.
Reitner J.M., Gruber W., Römer A., Morawetz R. (2010) - Alpine overdeepenings and paleo-ice flow changes: an integrated geophysical-sedimentological case study from Tyrol (Austria). Swiss Journal of Geosciences, 103, 385-405.
Rutter E., Brodie K., James T., Burlini L. (2007) - Large-scale folding in the upper part of the Ivrea-Verbano zone, NW Italy. Journal of Structural Geology, 29, 1-17.
Sacco F. (1892) - L'anfiteatro morenico del Lago Maggiore. Annali Reale Accademia d'Agricoltura di Torino, 43, 1-252.
Salmojraghi F. (1882) - Alcune osservazioni geologiche sui dintorni di Comabbio. Atti Società Italiana di Scienze Naturali, 25, 268-290.
Scapozza C., Castelletti C., Soma L., Dall'Agnolo S., Ambrosi C. (2014) - Timing of LGM and deglaciation in the Southern Swiss Alps. Géomorphologie: relief, processus, environnement, 20, 307-322. Doi: 10.4000/geomorphologie.10753
Seguinot J., Delaney I. (2021) - Last-glacial-cycle glacier erosion potential in the Alps. Earth Surface Dynamics, 9, 923-935. Doi: 10.5194/esurf-9-923-2021
Seguinot J., Ivy-Ochs S., Jouvet G., Huss M., Funk M., Preusser F. (2018) - Modelling last glacial cycle ice dynamics in the Alps. The Cryosphere, 12(10), 3265-3285. Doi: 10.5194/tc-12-3265-2018
Sergeev S.A., Steiger R.H. (1995) - Caledonian and Variscan granitoids of the Gotthard massif: new geochronological and geochemical results. Schweizerische mineralogische und petrographische Mitteilungen , 75, 315-316.
Schmid S.M., Pfiffner O.A., Froitzheim N., Schönborn G., Kissling E. (1996) - Geophysical-geological transect and tectonic evolution of the Swiss-Italian Alps. Tectonics, 15, 1036-1064.
Shilts W.W. (1982) - Glacial dispersal: principles and practical applications. Geoscience Canada, 9, 42-47.
Shilts W.W. (1993) - Geological Survey of Canada's contributions to understanding the composition of glacial sediments. Canadian Journal of Earth Sciences, 30, 333-353
swisstopo (2005) - Geological Map of Switzerland, 1:500.000; Federal Office of Topography, Wabern.
Turco F., Tartarotti P. (2006) - The Antrona nappe: lithostratigraphy and metamorphic evolution of ophiolites in the Antrona Valley (Pennine Alps). Ofioliti, 31, 207-221.
van Husen, D. (2004) - Quaternary glaciations in Austria. In: J. Ehlers, P. L. Gibbard (Eds.), Quarternary Glaciations-Extent and Chronology. Developments in Quaternary Science, 2, Part I: Europe, 401-412.
Višnjević V., Herman F., Prasicek G. (2020) - Climatic patterns over the European Alps during the LGM derived from inversion of the paleo-ice extent. Earth Planet Science Letters, 538, 116185.
Winterberg, S., Picotti, V., Willett, S.D., (2020) - Messinian or Pleistocene valley incision within the southern Alps. Swiss Journal of Geosciences, 113, 7.
Wirsig C., Zasadni J., Christl M., Akçar N., Ivy-Ochs S. (2016) - Dating the onset of LGM ice surface lowering in the High Alps. Quaternary Science Reviews 143, 37-50.

Ms. received: October 27, 2022 *Revised: November 22, 2022*
Accepted: November 25, 2022 *Avaiable online: December 22, 2022*